CHAPTER 16

Nano-scale Characterization of the Dynamics of the Chloroplast Toc Translocon

L. Evan Reddick,[*] Prakitchai Chotewutmontri,[†] Will Crenshaw,[*] Ashita Dave,[*] Michael Vaughn,[*,1] and Barry D. Bruce[*,†,‡]

[*]Department of Biochemistry
Cellular and Molecular Biology
University of Tennessee at Knoxville
Knoxville, Tennessee 37996

[†]Graduate School of Genome Science and Technology
University of Tennessee at Knoxville
Knoxville, Tennessee 37996

[‡]Department of Microbiology
University of Tennessee at Knoxville
Knoxville, Tennessee 37996

[1] Current Address: Department of Chemistry and Biochemistry, Arizona State University, Arizona

METHODS IN CELL BIOLOGY, VOL. 90

0091-679X/08 $35.00
DOI: 10.1016/S0091-679X(08)00816-9

Abstract

Translocons are macromolecular nano-scale machines that facilitate the selective translocation of proteins across membranes. Although common in function, different translocons have evolved diverse molecular mechanisms for protein translocation. Subcellular organelles of endosymbiotic origin such as the chloroplast and mitochondria had to evolve/acquire translocons capable of importing proteins whose genes were transferred to the host genome. These gene products are expressed on cytosolic ribosomes as precursor proteins and targeted back to the organelle by an N-terminal extension called the transit peptide or presequence. In chloroplasts the transit peptide is specifically recognized by the Translocon of the Outer Chloroplast membrane (Toc) which is composed of receptor GTPases that potentially function as gate-like switches, where GTP binding and hydrolysis somehow facilitate preprotein binding and translocation. Compared to other translocons, the dynamics of the Toc translocon are probably more complex and certainly less understood. We have developed biochemical/biophysical, imaging, and computational techniques to probe the dynamics of the Toc translocon at the nanoscale. In this chapter we provide detailed protocols for kinetic and binding analysis of precursor interactions in organeller, measurement of the activity and nucleotide binding of the Toc GTPases, native electrophoretic analysis of the assembly/organization of the Toc complex, visualization of the distribution and mobility of Toc apparatus on the surface of chloroplasts, and conclude with the identification and molecular modeling Toc75 POTRA domains. With these new methodologies we discuss future directions of the field.

I. Introduction

A. Chloroplast Origin and Role of Protein Translocation

A hallmark of eukaryotic cells is its remarkable compartmentalization. This compartmentalization is accomplished largely through the formation of membrane-delineated sub-compartments, known as organelles. The lipid bilayers, surrounding the organelle, present an obstacle for protein transport from the site of synthesis in the cytoplasm. Localized within these membranes are specialized-protein conducting molecular machines known as translocons. The architecture of these translocons have been characterized from many membranes, including the archebacterial plasma membrane (Van den Berg *et al.*, 2004), the yeast endoplasmic reticulum (Beckmann *et al.*, 2001), the outer membrane of mitochondria (Model *et al.*, 2008), and the outer membrane of the chloroplast envelope (Schleiff *et al.*, 2003). These translocons facilitate the selective and active transport of proteins across the lipid bilayer. Through a combination of cryoEM and X-ray crystallography, it is clear that these molecular machines are nanometer-sized complexes that can occur with a range of conformations, including individual monomers in the archebacterial plasma membrane (diameter of 4.0 nm), a dimeric, and/or trimeric triangular complex in yeast mitochondrial outer membrane (edge length of 14.5 nm), to a tetramer in the chloroplast outer membrane (diameter of ~14 nm).

In plant cells, the compartmentalization is even more complex since these cells have two semi-autonomous organelles, the mitochondria and the plastid. The plastid gains its name from its tremendous plasticity in form and function. One of these plastid subtypes is the chlorophyll containing chloroplast, which is the site of photosynthesis. The chloroplast is widely accepted to have evolved from an endosymbiotic event involving phagocytosis of a primitive cyanobacterium by an autonomous eukaryotic cell, ~1.6 billion years ago (Basu *et al.*, 2008). Following internalization, the ancestral cyanobacteria began a slow transfer of its genome to the nucleus, such that modern chloroplasts typically encode only ~100 genes. This is much less than the many thousand of genes encoded by existing cyanobacteria (Cavalier-Smith, 2003). Although evolution resulted in a minimal plastid genome, the plastid proteome has remained remarkably large and complex, with over 2000 gene products identified (Kleffmann *et al.*, 2006). The large plastid proteome is maintained via the process of posttranslational translocation of nuclear-encoded preproteins (Keegstra and Cline, 1999), which contain an N-terminal extension known as the transit peptide (tp) (Bruce, 2000). Two complexes, known as the translocons of the outer/inner chloroplast membrane, or *Toc* and *Tic* complexes, mediate chloroplast protein import (Fig. 1). Components of the Toc translocon, Toc34 and Toc159, both GTPase preprotein receptors, facilitate the unidirectional and highly specific protein import by recognizing and binding to the transit peptide.

While phylogenetic evidence may argue that many components of the Tic complex were derived from preexisting cyanobacterial proteins (Jarvis and Soll, 2001), the origins of the Toc GTPases are most likely eukaryotic; the other member

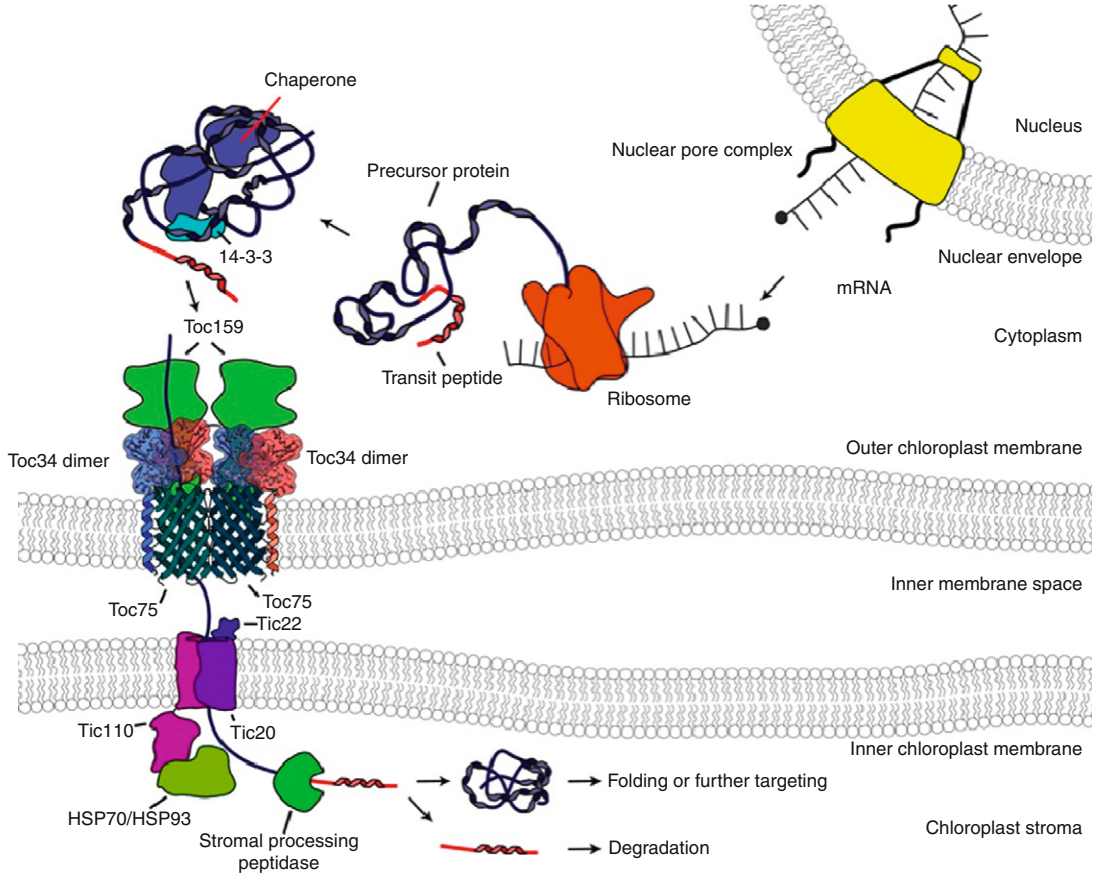

Fig. 1 Chloroplast protein import schematic. Genes encoding proteins destined for the chloroplast are transcribed in the nucleus where they must exit through the nuclear pore. This mRNA is translated on ribosomes into precursor proteins that have an N-terminal extension known as the transit peptide. The solubility and protease resistance of the precursor protein is maintained through the interaction of 14–3–3 proteins and chaperones where it is ultimately targeted to the chloroplast Toc translocon. Through the interaction of the receptor GTPases Toc159 and Toc34, the transit peptide drives the precursor protein entry through the beta-barrel protein Toc75 where it interacts with the Tic complex. The actions of cytosolic, IMS and stromal chaperones and Hsp proteins drive the import of the precursor protein using ATP. Stromal processing peptidase cleaves the transit peptide and the precursor protein folds to its ultimate active form, or proceeds to a suborganeller location for further import/processing. The tp is degraded via the presequence processing peptidase.

of the Toc complex, the β-barrel Toc75, is of prokaryotic origin (Reumann *et al.*, 1999). This prompted a recent postulation that the transit peptide has origins as a virulence factor, possibly excreted through the *Synechocystis* (PCC6803) β-barrel protein *Syn*Toc75 (Bolter *et al.*, 1998; Reddick *et al.*, 2007). Despite advances in identification of many of the components found in Toc and Tic, as well as the

availability of a low-resolution structure of the Toc apparatus (Schleiff *et al.*, 2003), the molecular mechanism of how preproteins are selected and translocated across both of these membranes is still very poorly understood.

Here, we introduce and discuss methods to quantitatively analyze the activity of this protein translocation process *in vitro*. This process can be distinguished into a binding step and a translocation step (Olsen *et al.*, 1989; Theg *et al.*, 1989), which differ in their energy requirements. *In organeller* experiments such as competitive chloroplast import and binding assays are powerful tools available for the quantitative measurement of chloroplast protein import. Here, we describe in detail the protocols for the import and binding competition assays based on *in vivo* labeled precursor of the small subunit of ribulose-1,5-bisphosphate carboxylase/oxygenase (prSSU) and reveal a new scintillation based method of quantitation that abrogates the need for chloroplast binding gel quantitation. These assays can be utilized to determine comparative affects of test subjects to prSSU import/binding. Through the use of fluorescently labeled antibodies, we can visualize a bound transit peptide to isolated chloroplasts. Additionally, following the identification of the receptor GTPases, Toc34 and Toc159, we have been able to express the soluble, cytosolic domains of these proteins in *Escherichia coli.* Using these recombinant proteins, we have now been able to develop very sensitive GTPase activity assays that allow the dynamics of these GTPase to be explored in detail using *in vitro* methods. We provide detailed methods for measuring both GTP binding, hydrolysis, and nucleotide exchange. Further aspects of the translocon organization and dynamics are revealed using a rapid native gel analysis that provides insight into the size and composition of the Toc apparatus. By utilizing a new technique, total internal reflectance fluorescence (TIRF), we can visualize intact chloroplasts and locate Toc complexes using fluorescent antibody techniques to determine the velocity and acceleration of the complexes on the chloroplast membrane. Finally, we have begun to use molecular modeling to provide structural insights of the Toc components based on crystallographic data from functionally related proteins. Using these models, we can now start to dissect the contributions of individual domains of Toc75.

B. Outline of Chapter

This chapter first addresses the production of chloroplast import substrates followed by rapid and reproducible chloroplast isolation techniques along with import and binding assays; included is a section on the quantitative analysis of data generated in said experiments. We also discuss novel methods of imaging the distribution of the ''active'' translocon by using Laser Scanning Confocal Microscopy (LCSM) and with appropriately fluorescent reporters, we can also observe the topology of a bound transit peptide within the translocon. Using BN-PAGE, 2-D PAGE, and western blotting, we demonstrate that the translocon itself is a dynamic apparatus, existing as an oligomer with multiple observed stoichiometries. Using total internal reflectance fluorescence microscopy (TIRFM), we can

visualize the mobility of individual Toc complexes in real time, and use particle tracking to observe the behavior of individual complexes. Finally, detailed kinetic analysis of the Toc associated GTPases is presented to dissect the properties of this molecular switch including nucleotide binding, hydrolysis, and exchange assays. Finally, with the availability of new membrane protein structures, we use molecular modeling to investigate the structure and function of β-barrel preprotein translocation channel, Toc75, and its associated soluble POTRA domains. A final concluding paragraph is offered to indicate future possible directions to investigate the structure and function of these nanoscale protein-conducting channels.

II. *In organeller* Chloroplast Import and Binding Assays

One of the powerful means of studying chloroplast protein import comes from the ability of perform *in organellar* assays using isolated and intact chloroplasts. These assays allow the design of very specific experiments where we can manipulate both the identity, the quantity of the precursor as either an *in vitro* translated product or as a chemically pure recombinant protein. In addition, we can further control the experiment by regulating the energy source by providing purified NTPs and by preventing photophosphorylation. We describe below the procedures for conducting both import experiments and binding experiments. By using ^{35}S-precursors and cold competitors, we can measure the affinity of the competitors for both binding and translocation.

A. Chloroplast Isolation

1. Prepare 2 Percoll step gradients in a 15 ml tube by carefully combining 2 ml of 80% Percoll in Import Buffer (IB; 50 mM HEPES–KOH pH 8.0, 330 mM Sorbitol) and 4 ml of 40% Percoll in IB, and keep on ice. Care in handling will prevent mixing and result in a sharper step gradient, and thus a better recovery of intact chloroplasts.
2. Harvest ~30 g of 12–14-day-old pea plants. Using scissors, coarsely chop the plants and further homogenize with a food processor in 3 short pulses (1–2 s each). Transfer to an ice-cold mortar; add 30 ml of ice-cold Grinding Buffer (GB; 50 mM HEPES–KOH pH 7.3, 330 mM Sorbitol, 1 mM $MgCl_2$, 1 mM $MnCl_2$, 2 mM EDTA, 0.1% BSA) containing about 0.3 g of sodium ascorbate and reduced glutathione.
3. Grind for 1–2 min, minimizing foam and filter through 1 layer of Miracloth on top of 1 layer of cheesecloth into a 50 ml tube. Centrifuge the filtrate at 900*g* for 5 min; decant the supernatant.

4. Resuspend the chloroplasts in 4–5 ml ice-cold IB with a natural bristle paintbrush. Gently paint the chloroplasts up the side of the tube until an even consistency is obtained.
5. Gently transfer the crude chloroplast suspension using a 14-gauge stainless steel cannula with a 10 ml plastic syringe onto the ice-cold Percoll step gradient (Fig. 2A) generated in step 1.
6. Centrifuge in a swinging bucket rotor at 3400*g* for 15 min with acceleration and deceleration set to medium. Two bands will form: an upper band of broken chloroplasts and thylakoids on top of the 40% Percoll and a lower band of intact chloroplasts at the interface of 40% and 80% (Fig. 2B). Carefully collect the intact chloroplasts with a syringe. Care should be taken to minimize the shear forces common with syringe manipulations.
7. With the same syringe, pull up about 3–5 ml ice-cold IB and gently resuspend the intact chloroplasts by inverting the syringe 3 times. Repeat steps 5–6.
8. Transfer the intact chloroplasts into a new 15-ml tube and pellet at 900*g* for 5 min.
9. Decant the supernatant and resuspend the intact chloroplasts in a minimal volume of ice-cold IB. Determine the chlorophyll concentration using Eq. (1) and by methods described previously (Arnon, 1949). We generally made about 0.4 mg of chlorophyll from 30 g of pea plants.

$$\text{mg/ml Chlorophyll} = \left[\frac{(8.02 \times A_{663}) + (20.2 \times A_{645})}{0.01\,ml \times 1000\,\mu g/mg}\right]$$

Eq. 1 Chlorophyll concentration calculation.

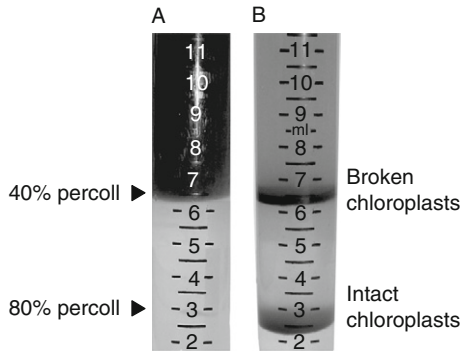

Fig. 2 Rapid isolation of intact chloroplasts. After tissue homogenization, filtration, and sedimentation, intact chloroplasts are isolated by centrifugation through a Percoll step gradient. The broken chloroplasts accumulate at the interface of the 40% Percoll whereas the intact chloroplasts collect on the 80% Percoll cushion.

Note: Care should be taken in the preparation of chloroplasts to minimize the overall time and keep all reagents on ice; proteases present in the cytosol will degrade the Toc proteins and result in semi-import competent chloroplasts. Further, the brushing and syringe, while requisite, will introduce shear forces and significantly contribute to the population of lysed chloroplasts if care is not taken to be gentle. Do not water the plants immediately prior to the harvest, as this water, albeit a small fraction will cause the buffers to become hypotonic and lead to chloroplast lysis. Finally, fresh preparation of GB and IB is not necessary, but due to the high sugar content in these buffers, they should be stored frozen, and thus will require thorough mixing prior to use due to the differential freezing rates of sugars and bulk water.

B. *In vivo* Radiolabeling of prSSU

1. *E. coli* BL21 (DE3) harboring the prSSU sequence in pET-11 vector is used (Klein and Salvucci, 1992) to inoculate 5 ml of Terrific Broth (TB) media containing 150 μg/ml ampicillin. Grow at 37 °C, 250 rpm, until OD_{600} 0.6 is reached.
2. Inoculate 3 ml of the culture into 30 ml of Dulbecco's Modification of Eagle's Medium (DMEM) deficient in methionine, cysteine, and glutamine containing 150 μg/ml ampicillin in a 50 ml tube.
3. When OD_{600} 0.6–0.8 is reached, induce with 1 mM IPTG; after 5 min of induction, 7 mCi of Trans ^{35}S-Label metabolic labeling reagent is added. Grow for 4–6 h.
4. Harvest the cells by centrifugation and wash twice with 15 ml of Buffer I (50 mM Tris–HCl, 2 mM EDTA, pH 8.0), resuspend in 15 ml of Buffer II (50 mM Tris–HCl, 2 mM EDTA, 0.5% TritionX-100, 1 mM DTT, pH 8.0). Lyse the cells by sonication, adding Benzonase to remove nucleic acids and lower the viscosity.
5. Collect inclusion bodies by centrifugation at 40,000*g* for 20 min. The inclusion bodies are then subjected to an extensive washing using a Dounce homogenizer. First, wash with 15 ml of Buffer II containing salt (300 mM NaCl), 4 times, and then wash with 15 ml of Buffer II, twice, followed by final wash with 15 ml of H_2O to remove salt and detergent.
6. Resuspend the inclusion body pellet in 300 μl of 8 M urea containing 50 mM DTT and 20 mM Tris–HCl, pH 8.0 and incubate with shaking overnight at 37 °C, 200 rpm. Most of the impurities are solubilized in this step. Centrifuge at 40,000*g* for 30 min to recover inclusion bodies.
7. Resuspend the inclusion body pellet again in 300 μl of 8 M Urea containing 50 mM DTT, 20 mM Tris–HCl, pH 8.0 with shaking at 37 °C, 200 rpm. The supernatant now contains the purified ^{35}S-prSSU. Insoluble impurities are removed by another centrifugation at 40,000*g* for 30 min. The supernatant can be stored at −80 °C.

C. Expression and Purification of prSSU and mSSU from Inclusion Bodies

The expression and purification of prSSU and mSSU proteins (Fig. 3, lanes 1 and 2) is accomplished by following the protocol listed in Section II.B., with the following variations Step 2, TB medium is used instead of deficient DMEM medium. The culture volume is scaled up to 50 ml in a 250 ml flask. Step 3, no labeling reagent is added. The volumes of buffers in step 4–5 are increased to 25 ml and the volumes of 8 M urea solutions in step 6–7 are increased to 500 μl. By employing the French Pressure Cell, we routinely achieve higher purity proteins; this is most likely due to sonic disruption of the inclusion body by sonication.

D. Expression and Purification of Transit Peptides

The standard IMPACT system (New England BioLabs) is used for expression and purification of all transit peptides (Fig. 3, lane 3). The transit peptide sequences are encoded on the pTYB2 plasmid, transformed into competent

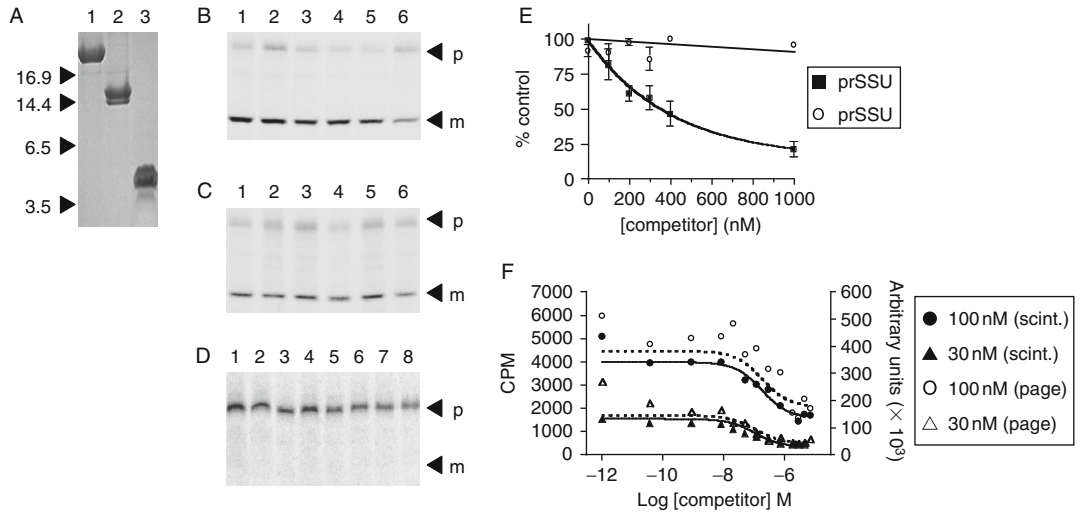

Fig. 3 Purified recombinant proteins and chloroplast Import and binding competitions. Panel A, Purified proteins used in chloroplast binding and import. Lane 1, purified prSSU, the precursor to the small subunit of rubisco. Lane2, mSSU, the mature form of prSSU is characterized by a smaller size due to the lack of the transit peptide. Lane 3, SStpNt, the small subunit transit peptide from *Nicotiana tobacum*. Panel B, SDS-PAGE digital autoradiograph of import competitions between 100 nM ^{35}S-prSSU and prSSU. Panel C is competition with mSSU; the competitors in lane 1–6 of both B and C are 0, 0.1, 0.2, 0.3, 0.4, and 1.0 μM cold competitor. Panel D, binding competitions between ^{35}S-prSSU and prSSU. The competitors in lane 1–7 are 0, 0.25, 0.5, 0.75, 1.0, 2.0, and 3.0 μM. Lane 8 is ^{35}S-prSSU loading control. Panel E, graphical analysis of import competition data generated from autoradiographs. Panel F, graphical analysis of binding competition data generated from autoradiograph (dashed line) and scintillation counting (solid line). Two concentrations of ^{35}S-prSSU were used, 30 and 100 nM. The K_d from autoradiograph and scintillation count are 31 nM and 91 nM, respectively.

ER2566 *E. coli* cells and induced via IPTG induction as fusion proteins with intein and chitin binding domains at the C-terminus of the expressed construct. Recombinant constructs are affinity purified on a chitin column and transit peptides are released by reductant mediated specific self-cleavage of the intein domain. By minimizing the preparation time and including protease inhibitor cocktails (PICs), one can prevent the loss of transit peptides to enzymatic degradation. The purified transit peptides are purified and stored as lyophilized powder at −80 °C. A recent publication details this procedure (Reddick *et al.*, 2007).

E. Chloroplast Import Competition Assay

1. The assay is performed in total volume of 300 μl. The reaction mixtures contain 100 nM ^{35}S-prSSU, 1 mM β-ME, 2 mM Mg–ATP, 0.5% BSA, 250 mM urea, and 0.125 mg chlorophyll/ml chloroplasts in the presence of IB with various concentrations of cold competitor. Stock solutions include freshly prepared 8 M urea solution (containing 20 mM β-ME, 20 mM Tris–HCl, pH 8.0), 1×IB, 2×IB, 100 mM β-ME, fresh 100 mM Mg–ATP, and 10% BSA. Prepare a set of 1.6 ml microfuge tubes containing 700 μl of 40% Percoll in IB for reisolation of the chloroplasts; keep everything on ice.
2. Resuspend the purified intact chloroplasts in IB containing 2% BSA, and adjust the concentration of chloroplasts to 1 mg chlorophyll/ml. Keep on ice.
3. Dilute ^{35}S-prSSU at least 2-fold with freshly prepared 8 M urea solution. Resuspend lyophilized transit peptide competitor in 8 M urea solution.
4. Pipette various concentrations of transit peptide competitor into fresh 1.6 ml reaction tubes. Add requisite volumes of 8 M urea solution into each tube to reach final concentration of 250 mM (take into account the urea in ^{35}S-prSSU and competitor solutions). When finished, every tube should contain an equal volume.

Note: It is important to not let the total urea concentration go above 350 mM. Urea levels above this lead to loss of import activity through some disruption of the chloroplast.

5. Prepare a ''master mix'' of IB, β-ME, Mg–ATP, BSA, and ^{35}S-prSSU for all reactions.
6. Pipette equal volume of the master mix into each tube, mix by vortex, and equilibrate the temperature by incubation at room temperature for 10 min.
7. To start the assay, add 37.5 μl of chloroplasts (Step 2) to each tube. Gently mix by inverting the tube 5 times. Incubate at room temperature for 15 min (mix occasionally by inverting 1 time).
8. Stop the reactions by adding 700 μl of ice-cold IB, mix, and keep on ice in the dark.
9. Reisolate the intact chloroplasts by overlaying the reaction solution on top of the 40% Percoll. Centrifuge in a swinging bucket rotor at 3400*g* for 5 min with acceleration and deceleration set to medium. Intact chloroplasts will

pellet at the bottom of the tube, broken chloroplasts and free ^{35}S-prSSU will remain at or above the interface.

10. Remove the broken chloroplasts and the Percoll. Gently resuspend the pellet in 1 ml of ice-cold IB using a Pasteur pipette and remove a 50 μl aliquot for quantification of the total protein using the BCA protein assay. Pellet the remaining 950 μl by centrifugation at 12,000*g* for 1 min.
11. Aspirate the supernatant and resuspend the pellet in 60 μl of ice-cold H_2O. Add 40 μl of 4× SDS sample buffer mix and boil for 4 min. From the result of BCA protein assay, equalize the protein concentration of all tubes using 2× SDS sample buffer.
12. For analysis, run 50 μl of the samples on a 10–20% SDS-PAGE gradient gel at constant 8 mA overnight. Dry the gels and place on phosphor screen for 3–24 h. The digital autoradiograph is acquired by scanning the screen with Storm Phosphorimager; ImageQuant software is used for quantification of the bands (Fig. 3B and C).

The same cautions and concerns (presented at the end of Section II.E., Chloroplast Import Assay) apply to the import competition assay. Intact chloroplasts should be prepared in parallel to minimize proteolysis. Freshly prepare urea to ensure the full solubilization of prSSU.

F. Chloroplast Binding Competition Assay

1. The assay is performed in total volume of 300 μl. The reaction mixtures contain 100 nM ^{35}S-prSSU, 10 mM DTT, 100 μM Na–ATP, 2 mM $MgCl_2$, 1% BSA, 300 mM urea, and 0.25 mg chlorophyll/ml chloroplasts in the presence of 1× IB with various concentrations of cold competitor. Stock solutions include freshly prepared 8 M urea solution (containing 50 mM DTT, 20 mM Tris–HCl pH 8.0), 1×IB, 2×IB, 100 mM DTT, fresh 10 mM Na–ATP, 100 mM $MgCl_2$, and 10% BSA. Prepare a set of 1.6 ml tubes containing 700 μl 40% Percoll in IB for reisolation of the chloroplasts; keep on ice.
2. To minimize the internal ATP in the chloroplast, the pea plants are harvested at the end of the dark cycle and chloroplast isolation is performed under dim light. The purified intact chloroplasts are resuspended in IB containing 2% BSA at the concentration of 1 mg chlorophyll/ml. Keep in the dark and on ice.
3. Dilute ^{35}S-prSSU at least 2-fold with freshly prepared 8 M urea solution to final concentration of 6 mM (6 μl will be used in each reaction). Resuspend lyophilized transit peptide competitor in 8 M urea solution. Generate serial dilutions of the competitor in 8 M urea solution (5 μl will be used in each reaction).

Note: It is important not to let the total urea concentration go above 350 mM. Urea levels above this will lead to loss of binding activity through some disruption of the chloroplast. By adding the urea denatured precursors last, we prevent them from precipitation upon dilution.

4. Prepare a master mix of required IB, DTT, Na–ATP, $MgCl_2$ BSA, and urea for all reactions (in total volume of 214 μl for each reaction)
5. Pipette 214 μl of the master mix into a set of new 1.6 ml reaction tubes, equilibrate the temperature by incubation at room temperature for 10 min.

Note: The following steps are performed under dim light to minimize ATP synthesis. Add 75 μl of chloroplasts to each tube. Gently mix by inverting the tube 5 times.

6. To start the assay, 6 μl of ^{35}S-prSSU and 5 μl of competitor are added in rapid succession. Gently mix by inverting the tube 5 times. Incubate at room temperature for 25 min (mix occasionally by inverting 1 time).
7. Follow steps 8–12 of the chloroplast import competition assay.
8. For analysis by liquid scintillation, 30 μl of the samples are bleached by adding 90 μl of 30% H_2O_2 and incubated at 80 °C for 30 min. Transfer bleached samples to a scintillation vial containing 2–4 ml Scintillation fluid and count.

G. Analysis Precursor Binding and Import

The process of precursor import can be broken down into a binding process and an import process. Using radiolabeled preproteins, it is possible to quantitate these steps into the number of molecules/chloroplast/min bound or imported as described above. The import data is acquired by quantifying the imported ^{35}S-prSSU by first running and subsequently drying an SDS-PAGE gel and subjecting it to a Phosphorimager. SDS-PAGE is required to separate the bound ^{35}S-prSSU from the imported ^{35}S-prSSU (processed to mSSU) labeled as p and m in Fig. 3B and C. As the name implies, import is prevented in the binding assay (II.F) and no bands of imported ^{35}S-prSSU are detected on the gel (Fig. 3D). This allows direct quantification using liquid scintillation counting without running SDS-PAGE to separate the species.

The import experiment generates data that can be fit with linear regression (competitors that do not compete, i.e., mSSU) while a one phase exponential decay fits data with competitors that do compete (prSSU). With the exponential decay fit, we can determine the IC_{50} for the competition import data (Fig. 3E). Varying the concentration of the radioactive prSSU with other variables held constant generates two sets of competitive binding data that can be globally fit using the GraphPad Prism program. The binding data are fit to a homologous binding event to determine the dissociation constant (K_d) and maximum number of binding sites (B_{max}, Fig. 3F). Analysis of competitive binding data of ^{35}S-prSSU with other proteins will determine the equilibrium dissociation constant (K_i) of the competitor. By comparing data in Fig. 3F fit to solid lines (closed circles and triangles, left y-axis, data from scintillation counting) and data fit to dashed lines (open circles and triangles, right y-axis, data from Phosphorimager analysis) scintillation analysis provides excellent data with a higher signal-to-noise ratio over

Phosphorimager data; a Pearson correlation test reveals a correlation of 0.978. This argues against the need to run gels and subject them to Phosphorimager analysis.

H. LSCM Imaging of the Bound Transit Peptide

The orientation and interaction of the transit peptide at the surface of the chloroplast is of importance, especially in light of the binding and import data. We have previously described a dual-tagged transit peptide His-S-SStp, which interacts with the Toc apparatus with the same affinity as the WT peptide yet accumulates in the Toc translocon (Subramanian *et al.*, 2001). This construct allows us to detect the short S-tag using a high affinity, monovalent S-protein detection system that can be FITC coupled for microscopy (Kim and Raines, 1993). Using this system, we created several C-terminal deletion constructs of the transit peptide (Fig. 4A). Additionally, using antibodies against the full length transit peptide, we confirmed the position of the cross-reacting epitope that was predicted to be located at the C-terminal portion of the transit peptide (Fig. 4B). Using these truncations, we observe that Δ25 and Δ36 but not Δ5 of SS-tp lose cross-reactivity (Fig. 4C) identifying the reactive epitope shown in yellow. Coomassie stained lanes 1–4 and anti-SStpNt lanes 5–8 refer to the truncations in A and their slight mobility difference is reflective of their deletions. Using S-protein FITC, we observe a punctate distribution of the transit peptide associated with the Toc apparatus. An identical labeling pattern was observed when we used the FITC coupled anti-SS-tp antibodies indicating that both the N-terminus and the C-terminus of the bound transit peptide are concurrently accessible to the cytosolic face of the chloroplast. Dual labeling using two different fluorescent detections indicates that these two detections colocalize to the same particle within the resolution of technique (data not shown). These results suggest that at least for this transit peptide construct, the conformation of the bound transit peptide is such that both the N- and C-terminus remain exposed to the cytoplasm (Fig. 4D).

III. Toc Translocon Dynamics

A. Solubilization of Intact Translocons and Dissociation of the Toc Complex

Our laboratory has revealed many features of the heterologously expressed, recombinant, purified Toc components through both standard and advanced experimentation (Reddick *et al.*, 2007). However recently, we have developed and refined existing methods including Blue Native PAGE (BN-PAGE) and 2D-PAGE (Fig. 5A-C). BN-PAGE is a charge shift technique developed by Schagger and von Jagow to separate native membrane multiprotein complexes (Schagger and von Jagow, 1991). These membrane protein complexes are solubilized by a minimal amount of a neutral detergent such as Triton X-100, *n*-decyl-maltoside, or digitonin (Eubel *et al.*, 2005), and a negative charge is induced by the binding of Coomassie blue

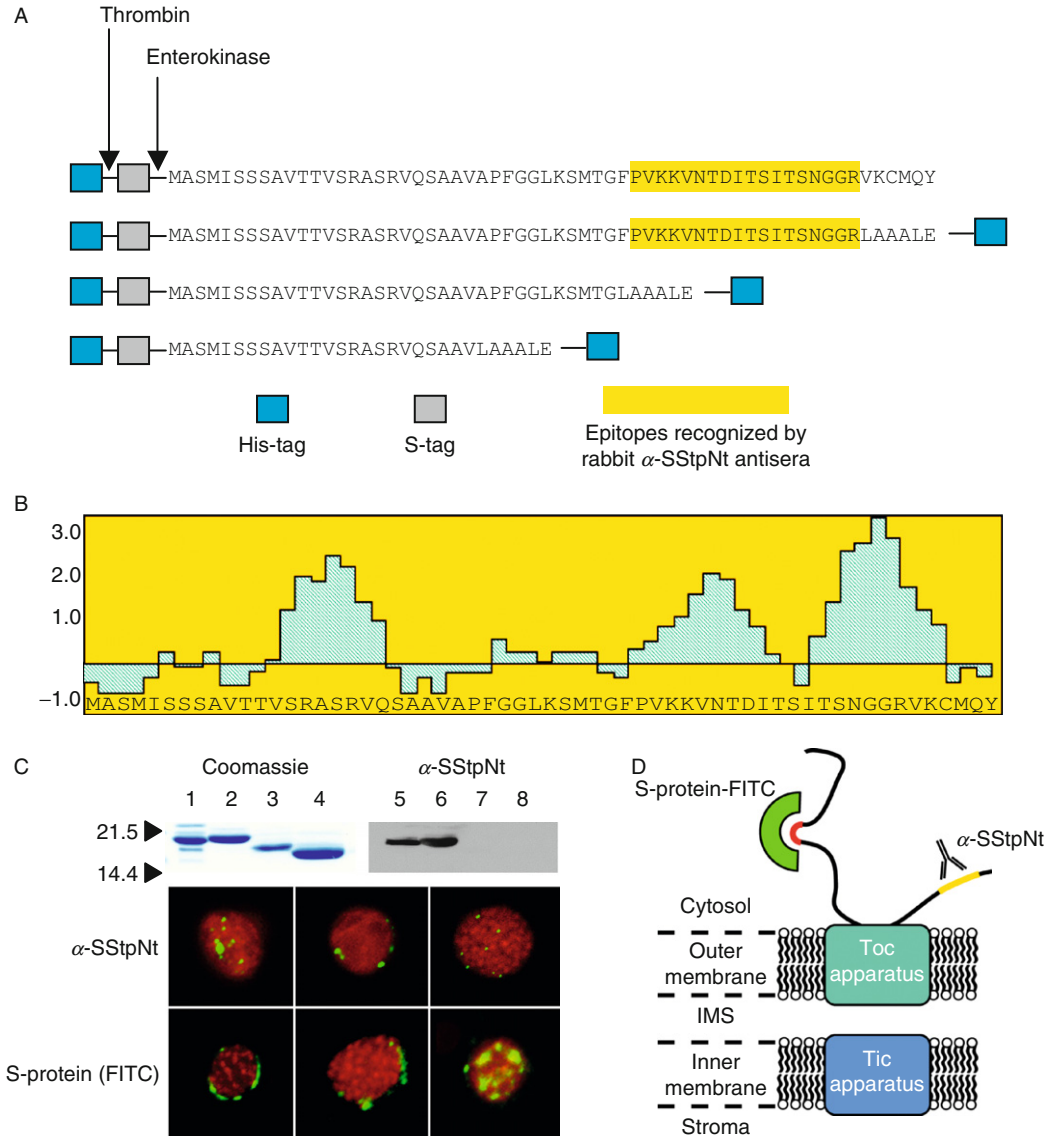

Fig. 4 Mapping the topology of a bound transit peptide in the Toc translocon. Panel A, Sequences of full length and C-terminal deletion mutants of His-S-SStp (Subramanian *et al.*, 2001) and placement of the dual-epitope tags (His-tag and S-tag). Panel B, Plot of predicted antigenicity of the SS-tp using the Hopp and Wood algorithm in DNAstar Protean software. Panel C, Top indicates the CBB stained SDS-PAGE gel and Western Blots of the His-S-SStp deletions, mapping the location of the dominant epitope recognized by our rabbit anti-SStpNT antibody to the C-terminus. Lower images show three representative chloroplasts with a bound His-S-SStp fluorescently labeled with either (1) a FITC-conjugated GAR secondary antibody (top three) or (2) a FITC-conjugated S-protein that reacts with the N-terminally placed S-tag. Panel D. Model indicating the topology of the bound transit peptide with both the C and the N-termini of the bound His-S-SStp are exposed to the cytosol.

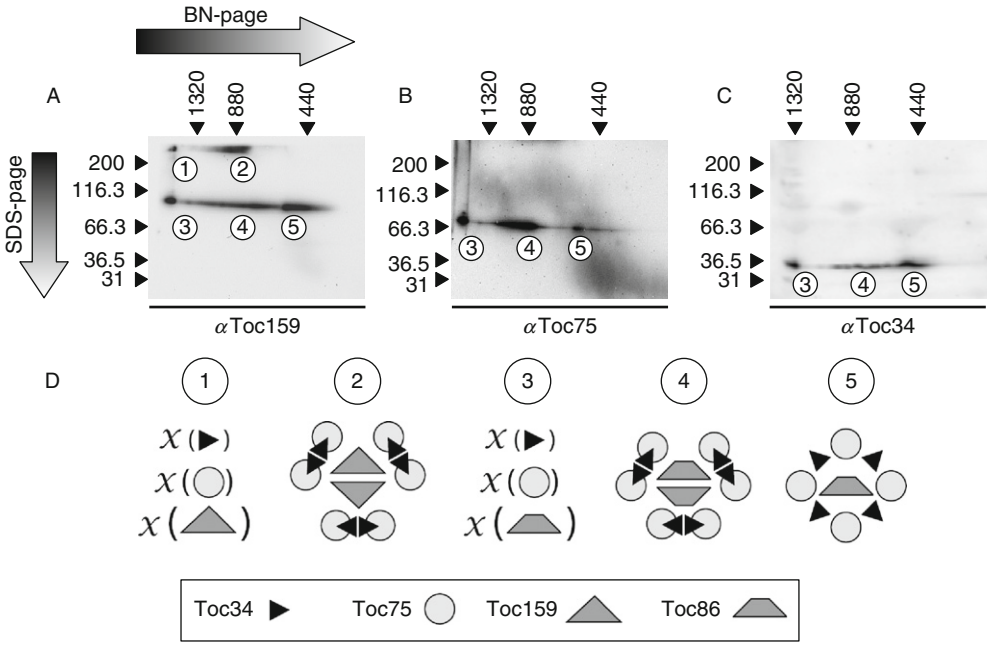

Fig. 5 2D-PAGE analysis of Toc translocon dynamics. The horizontal arrow above the gel represents the direction of electrophoresis in the Blue Native PAGE (1st dimension) and the vertical arrow represents the direction of electrophoresis in the SDS-PAGE (2nd dimension) in A–C. Molecular weight markers are presented above and to the left of each blot. Panel A–C represent the western analysis of intact chloroplast 2-D PAGE using antibodies against Toc159 (A), Toc75 (B), and Toc34 (C). Presumably, a Tic–Toc supercomplex has difficulty migrating into the BN-gel and therefore the stoichiometry of Toc34, Toc75, and Toc159 is questionable in number 1. A complex of 6:6:2 Toc34:Toc75:Toc159 is seen in 2. Degradation is a common aspect of chloroplast preparations, and the majority of Toc159 is present as Toc86 in 3–5. The possible stoichiometries are unknown (3), 6:6:2 (4) and 4:4:1 (5). In panel D, complexes 1 and 3 are represented as unknown stoichiometries of Toc34, Toc75, and Toc159 (1) whereas the degradation product Toc86 is present in 3. Numbers 2, 4, and 5, presented from the perspective of looking down upon the chloroplast outer membrane, represent the following stoichiometries: 6:6:2 (Toc34:Toc75:Toc159); 4, 6:6:2 (Toc34:Toc75:Toc86); 5, 4:4:1 (Toc34:Toc75:Toc86). From the intensities present, we conclude that the 6:6:2 stoichiometry is favored over 4:4:1.

G-250 to the hydrophobic domains on the surface of proteins; the use of Coomassie to both abrogate hydrophobic collapse and concomitantly stain the protein(s) is of beneficial significance. Initial runs should be performed on steep gradient gels (~4–20%), as uniform gels will not be satisfactory (Schagger *et al.*, 1994).

Previously, researchers purified the Toc core complex from outer envelope membrane vesicles by *n*-decyl-*β*-maltoside solubilization followed by sucrose density gradient centrifugation. The core complex was analyzed by size exclusion chromatography, was determined to contain the 86-kDa fragment of Toc159, Toc75, and Toc34, and eluted at around 500 kDa. The stoichiometry of the core complex was

determined to be 1:4:4–5 between Toc159, Toc75, and Toc34 giving a calculated molecular mass of ~522 kDa (Schleiff *et al.*, 2003); however, this reported stoichiometry might be the result of the experimental conditions. BN-PAGE has been utilized to characterize the mitochondrial import machineries (Dekker *et al.*, 1996, 1998; Meisinger *et al.*, 2001) as well as the Tic complex (Caliebe *et al.*, 1997; Kuchler *et al.*, 2002). Kikuchi *et al.* recently reported that the intact Toc complex, solubilized from intact chloroplasts, has an observed molecular mass of 800–1000 kDa, and contains at least Toc159, Toc75, and Toc34 (Kikuchi *et al.*, 2006). Further, Chen and Li have reported that during active import, precursors interact with two complexes: an 880-kDa Toc complex and a 1320-kDa complex containing the Toc components as well as Ticl 10, Hsp93, and an Hsp70 homolog, before associating with the Tic/Toc supercomplex, which is too large to be analyzed by BN-PAGE (Chen and Li, 2007). Analysis of western blot hybridization of BN-PAGE and 2D-PAGE of the core Toc complex will allow for the observation of organizational and dynamic changes induced by the incubation of nucleotides, preproteins, and exogenously added Toc components to purified chloroplasts.

B. Blue Native PAGE of Intact Chloroplast for Analysis of Toc Assembly

1. Follow the chloroplast isolation protocol above in II A, steps 1–8 with the following modifications: To all buffers add 5 μl/ml PIC for plant cell and tissue extracts, Sigma P-9599 except GB and solubilization buffer (SB, 1% digitonin in 50 mM BisTris–methane pH 7.0, 500 mM aminocaproic acid, 10% glycerol) to which add 10 μl/ml PIC.
2. Resuspend the pellet in 1 ml IB, divide into three 1.6 ml microfuge tubes.
3. Make 700 μl of a 2× solution in IB of the nucleotide or protein to be tested for complex dissociation. Keep chloroplasts in the dark, and mix 330 μl of the experimental solution with one tube of chloroplasts to start the longest time point incubation. After 15 min, repeat for the second time point, and mix 330 μl of IB with the control chloroplasts.
4. After 15 min, repurify intact chloroplasts over 500 μl of 40% Percoll. Aspirate the Percoll, supernatant, and broken chloroplasts, leaving a pellet of intact chloroplasts.
5. Resuspend intact chloroplasts in 175 μl of SB and solubilize for 10 min on ice in the dark. Remove insoluble material by ultracentrifugation at 100,000*g* for 10 min.
6. Decant supernatant and mix with Coomassie G-250 solution (5% Brilliant Blue G-250, 50 mM BisTris, 500 mM aminocaproic acid) to achieve an 8:1 detergent to Coomassie ratio.
7. Load and run a 0.75 mm thick 4–10% polyacrylamide gradient gel containing 50 mM BisTris and 500 mM aminocaproic acid for 5 h at 200 V at 4 °C. BSA (66 and 132 kDa) and Ferritin (440, 880, and 1320 kDa) are used as molecular weight markers.

8. Cut-off lane containing markers and stain (general Coomassie staining protocol). Separate individual lanes and heat at 65 °C in buffer containing 3.3% SDS, 4% βME, and 65 mM Tris–HCl pH 6.8 for 20 min.

C. 2D SDS-PAGE and Western Blot Analysis

1. Pour a 1.5 mm 8–16% SDS-PAGE gradient gel and allow polymerization. Overlay ~1 ml of 4.8% stacking gel on the gradient gel, top with 50% isopropanol, and allow polymerization.
2. Remove a strip of a BN-PAGE gel as per section B, step 8 above and gently place it horizontally above the stacking gel. Pour 4.8% stacking gel around the BN-PAGE lane and a small, one well comb (for molecular weight markers) to seal the gel slice in place. Allow polymerization.
3. Run the gel at 30 mA for ~1 h until the dye front has run off.
4. Transfer proteins from gel to Immobilon PVDF using a Genie electrophoretic transfer apparatus (Idea Scientific) for 4 h at 4 °C. The choice of transfer buffer will depend on your choice of analysis parameters: For western blotting against Toc75 and Toc159, transfer in high molecular weight transfer buffer (48 mM Tris, 390 mM Glycine, 0.1% SDS, 20% methanol). For western blotting against Toc34, use high pH transfer buffer (100 mM Tris, 192 mM Glycine, 20% methanol).
5. Block the Immobilon with TBST (25 mM Tris–HCl pH 8.0, 137 mM NaCl, 3 mM KCl, 0.1% Tween 20) containing 3% nonfat milk and 0.5% BSA for 1 h. All incubations can be carried out at room temperature with rocking.
6. Incubate the 1° antibody with the blots for 2 h at 1:25,000.
7. Wash blots for 10 min, 3 times with TBST.
8. Incubate the 2° antibody with the blots for 1 h at 1:25,000, repeat step 7.
9. Incubate blots with chemiluminescent substrate (HRP) and photon count on a Chemidoc system (BioRad).
10. Analyze blots with Quantity One software (BioRad) and quantitate the complexes formed at different sizes.

Figure 5 details the western results obtained by the previous protocol. BN-PAGE separates the complexes while SDS-PAGE separates the individual proteins for easy identification and correlation with the native size of the complex with which a given protein is associated. In panel A, antibodies against Toc159 indicate that this protein exists as both Toc159, numbers 1 and 2, and Toc86, numbers 3–5. Numbers 1 and 3 refer to complexes in which the stoichiometry is unknown, indicated by an X before the representative cartoon in D. The stoichiometry is unknown due to the large size of the complex in the first dimension (greater than 1320 kDa). Number 2 represents the migration of a 6:6:2 (Toc34:Toc75:Toc159) complex whereas number 4 represents a similar 6:6:2 with Toc86, the more

proteolytically resistant form of Toc159. Number 5 in panel D represents a stoichiometry of 4:4:1, again with Toc86. Panels B and C underscore this distribution by using antibodies against Toc75 and Toc34, respectively.

D. TIRF Imaging of Toc Dynamics

TIRFM allows for the excitation of fluorophores only within the cell surface, leading to very low background fluorescence and yielding a high signal-to-noise ratio. An evanescent field is produced by the total internal reflection of the excitation beam. Proximal fluorophores will be excited within this evanescent field without exciting more distant fluorophores (Axelrod, 2001). TIRFM allows for the observation of single fluorescent molecules and the study of their dynamics and kinetics while cellular photodamage and photobleaching are minimized (Toomre and Manstein, 2001). In contrast, TIRFM allows for the illumination of <100 nm from the surface, whereas confocal systems typically show an optical section of $\sim$500–800 nm. Toc159 on the surface of intact chloroplasts is labeled with fluorescent antibodies allowing the real time visualization of the dynamic environment of this translocon component while minimizing the effects of chlorophyll autofluorescence. The following general protocol details the preparation of chloroplasts for TIRFM analysis.

1. Block purified intact chloroplasts with 1% BSA in IB with rocking for 30 min.
2. Incubate the 1° antibodies with the chloroplasts for 1 h with rocking at a titer of 1:500.
3. Wash by carefully injecting 40% Percoll under the chloroplasts, centrifuge for 10 min at 3400*g*, and resuspend in IB containing 1% BSA. Perform this wash for a second time.
4. Incubate the 2° fluorescent antibodies with the chloroplasts for 1 h with rocking at a titer of 1:500.
5. Repeat step 3.
6. Labeled chloroplasts are then visualized on a Nikon TIRFM.

In the future, this technique shows promise for the labeling of multiple Toc components with different fluorophores and analyzing the kinetic and dynamic properties of the Toc complex through the utility of various excitation and emission wavelengths. Presently, we have used this technique to visualize intact chloroplasts that have been immunodecorated with fluorescent antibodies against atToc159 which can be viewed in bright field and subsequently deconvoluted, Fig. 6A and B, respectively. Using Nikon particle tracking software, we can follow individual labeled translocons on the chloroplast surface and calculate their mobility. Panels C–E represent different chloroplasts on which a fluorescent spot has been selected and its velocity and acceleration as a function of time has been determined and graphed. Interestingly, like most single molecule detections, we observe a discontinuity in mobility, with relatively long periods of stasis

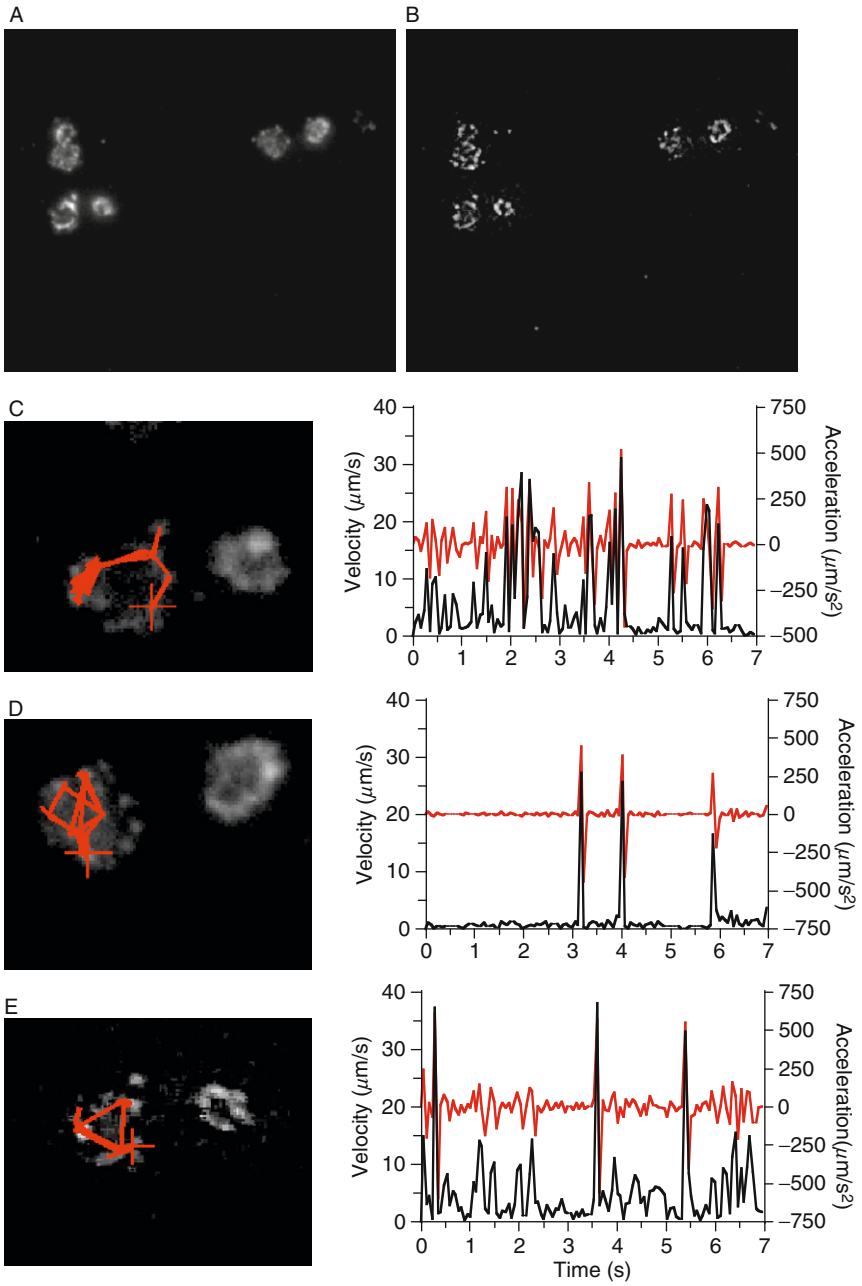

Fig. 6 TIRF microscopic analysis of Toc159 dynamics. Panel A and B is a wide field image of isolated chloroplasts immunodecorated with anti-Toc159 antibodies. Deconvolution using the bundled Nikon software yields the image in panel B in which dynamic background subtraction has been performed. Panels C–E represent isolated chloroplasts in which an isolated fluorescent spot has been selected and both velocity and acceleration have been determined as a function of time (associated graph to the right).

punctuated by short bursts of mobility. In the future, this technique allows us to monitor the association/dissociation dynamics of individual translocon subunits by utilizing multi-color immunolabeling with anti-Toc34, anti-Toc75, and anti-Toc159 antibodies. Additionally, by varying the nucleotide and preprotein/transit peptide status, we can determine whether the energetics and translocation activity alter its mobility and subunit composition.

IV. Activity and Enzymology of Toc GTPases

GTPase proteins have historically low basal hydrolytic rates, existing in either a GDP (off) or a GTP (on) state in order to function as molecular switches rather than molecular motors (Bourne *et al.*, 1990, 1991). This basal hydrolytic rate can be stimulated through the interaction of regulatory proteins, such as GTPase Activating Proteins (GAP) and Guanine nucleotide Exchange Factors (GEF) (Bos *et al.*, 2007). GAPs are generally specific for their target GTPase acting to accelerate the rate of hydrolysis, effectively turning the switch "off." Recently, we showed that the transit peptide is the GAP for psToc34 (Reddick *et al.*, 2007). A GEF catalyzes the dissociation of bound GDP from the GTPase effectively turning it "on." A GEF acts through interaction either directly with the GTPase switch domains, or allosterically at an auxiliary location to lower the affinity for nucleotide, such that GTP, largely through mass action, replaces GDP; the cellular concentration of GTP is several times greater than that of GDP (Vetter and Wittinghofer, 2001). Here, we describe in detail the methods used to quantitatively measure the hydrolytic rates of isolated Toc proteins *in vitro*, determine the K_d and K_i through competitive nucleotide binding experiments and carefully measure the rate of GDP/GTP exchange.

A. Purification of Toc Proteins

The growth and purification of Toc proteins from *E. coli* follows standard bacterial culture techniques. Briefly, the cDNA encoding the truncated, soluble domains of the Toc proteins were inserted into pET hexahistidine tag vectors and transformed into competent BL21(DE3)-RIL *E. coli* cells by standard procedures. The cells are grown at 37 °C with shaking to an $O.D._{600}$ of 0.5 at which time they are induced with 1 mM IPTG, after which the cells are harvested via centrifugation. Cells are lysed via French Pressure Cell; supernatant and pellet are separated via centrifugation and psToc34 protein is purified using the PrepEase system (USB Corp., Cleveland, Ohio). Protein is eluted and quantitated. (For further information, please refer to Reddick *et al.*, 2007.)

B. GTP Hydrolysis Assay

In order to determine the rate of hydrolysis of these GTPases, a highly quantitative hydrolysis assay was developed. This was done due to the fact that an assay of this kind was not available. This assay relies on the enzymatic release

of a radiolabeled γ-$^{32}P_i$ from [γ-^{32}P]GTP and its subsequent isolation and quantitation to determine the enzymatic activity of the Toc protein. A 96-well plate will be used for this assay such that column 1, rows A–H will be the reaction wells and columns 2–6, rows A–H will be the quenching wells for column 1 at five aliquot removal time points. An additional assay with varying parameters or a duplicate of the current assay can be carried out in column 7 with quenching wells in columns 8–12. Column 1, rows A–H will have a final total volume of 100 μl and will be composed of three parts: (1) cold GTP solution, (2) radioactive GTP solution, and (3) Toc protein solution. The addition of Toc protein solution to the well will start the reaction, and thus the timing of aliquot removals. Aliquots of 15 μl will be removed at precise times from each well in column 1 and added to specific wells (rows 2–6, A–H), which will contain 200 μl of quenching suspension (10% (w/v) activated charcoal suspension in 100 mM HCl and 5 mM H_3PO_4). The acids are present to stop the reaction and reduce spontaneous hydrolysis while the activated charcoal can remove from solution the carbon containing compounds, leaving inorganic phosphate, buffer components, acids, and water. The assay wells are put together as per the following protocol; wells are denoted by their grid number and corresponding letter (e.g., 1E refers to the well in column 1 at row E):

Part 1: Cold GTP Solution

1. Add 3.3 μl 10× GBS (200 mM Tricine–KOH, pH 7.65, 10 mM $MgCl_2$, 500 mM NaCl, 10 mM βMe) to each well (1A–H) along with 30 μl ddH_2O to 1A.
2. Add 0.3 μl of 33.3 mM GTP and 27.7 μl ddH_2O to 1B.
3. Add 1.5 μl 33.3 mM GTP and 28.5 μl ddH_2O to 1C. 1D–1H will have 3, 7.5, 15, 22.5, and 30 μl 33.3 mM GTP solution with the requisite volume of ddH_2O to bring the total volume of part 1 to 33 μl.

This ensures that during the assay, rows A–H will have 0, 1, 5, 10, 25, 50, 75, and 100 μM cold GTP creating the substrate titration curve necessary for Michaelis–Menten kinetic measurements.

Part 2: Hot GTP Solution

1. Add 1.76 μl 10 nM [γ-^{32}P]GTP (800 Ci/mmol) and 0.01 mCi/μl) to 14.66 μl 10× GBS and 130.24 μl ddH_2O to create a final volume of 146.66 μl of radioactive GTP solution in a 1.6 ml microfuge tube.
2. Add 16.66 μl of this solution to wells 1A–H.

Part 3: Toc Protein Solution

1. Add 22.76 μl of 5 mg/ml Toc protein to 44 μl 10× GBS and 373.24 μl ddH_2O.

This solution is the "start" solution, as its addition to wells in column 1 of the 96-well plate will start the reaction.

Part 4: GTP Hydrolysis Assay

1. At time equals 0:00 (min:s), add 50 μl ddH_2O to 1A.
2. At 0:15, add 50 μl Part 3 to 1B.
3. At 0:30, 50 μl Part 3 to 1C; 0:45, 1D; 1:00, 1E; 1:15, 1F; 1:30, 1G; 1:45, 1H.
4. At 5:00, remove 15 μl from 1A and place it into 2A.
5. At 5:15, remove 15 μl from 1B and place it into 2B; 5:30, 15 μl from 1C to 2C, etc.
6. At 10:00, remove 15 μl from 1A and place into 3A; 10:15, 15 μl from 1B to 3B, etc.

Columns 2–6 represent the 5, 10, 15, 20, and 25-min time points for each of the reaction wells. Once the last aliquot is removed and added to the activated charcoal, use a multichannel pipettor to vigorously mix the contents of all wells, being careful to avoid well-to-well contamination.

7. Transfer the contents of wells 2–6, rows A–H to a 96-well 0.2 μm filter plate. Place in a 96-well vacuum manifold, and apply vacuum.

This will transfer the liquid content to the receiving plate below, while retaining the charcoal. This step effectively separates unhydrolyzed [γ-^{32}P]GTP from $^{32}P_i$.

8. Place 100 μl MicroScint 40 scintillation fluid into wells 2–6, A–H of a TopCount MicroScintillation Plate (Perkin Elmer). Transfer 20 μl of the radioactive filtrate from each well to the corresponding well in the scintillation plate, pipetting vigorously to ensure even distribution of aqueous material in the scintillant.
9. A TopSeal sealing film is applied to the top of the scintillation plate which is placed into a TopCount NXT Microplate Scintillation Counter, Perkin Elmer Life Sciences. Scintillation counting should be performed for (at minimum) 5 min/well and cross talk filters applied.

There are several factors that one must determine in order to calculate the activity of the enzyme; according to Michaelis–Menten kinetics, this rate is reported as mole substrate consumed or hydrolyzed per unit time per mole enzyme. Equation (2) shows the general formula needed to transform scintillation counts into enzyme activity, and in our case, has been incorporated into a Microsoft Excel spreadsheet. First, counts per minute are graphed as a function of time generating a CPM versus Time plot for each substrate concentration along with a spontaneous hydrolysis rate that should be subtracted from the rate of hydrolysis prior to analysis. The slope of this line will represent ΔCPM/min, or C_m. The isotope per time point, I_m, must be determined; it is simply the isotope concentration in the reaction multiplied by the volume of each time point aliquot. Determine the ratio of your stock cold GTP to the volume of cold GTP in each reaction. The hot ratio is also determined in the same manner by taking the ratio of the [γ-^{32}P]GTP stock (MP Biomedicals) to the actual volume of hot GTP in each reaction. The cold:hot ratio (R_{GTP}) is simply the ratio of these two ratios. Next, S_f is the scintillation fraction factor, or the reciprocal of the scintillation sample volume divided by the sum of the HCl–charcoal volume and the time point volume. Since CPM is not

directly related to a scintillation event, only DPM, or disintegrations per minute, one must convert CPM to DPM. This is accomplished by multiplying the Ci per time point (which is determined by multiplying the Ci concentration in the reaction by the time point volume) by 1 Ci (expressed as 2.22×10^{12} dpm) to give D_m. The number of Toc molecules, M_{Toc}, is determined by dividing the product of the volume of enzyme in each reaction and the stock mg/ml of enzyme by the molecular weight of the enzyme. The HCl–charcoal dilution factor, or C_{dil}, is determined by dividing the time point volume by the sum of the time point and the HCl/charcoal volume. The counting efficiency, C_{eff}, and isotope purity factor, P_f, are determined empirically and by contacting the manufacturer of the radionucleotide, respectively.

Once all of these parameters have been determined and placed into a spreadsheet, the assay is very simple and highly reproducible, save pipetting errors by the experimenter. With each concentration of substrate, this spreadsheet will generate a single data point, expressed as mol GTP hydrolyzed per unit time per mol enzyme. In this case, we have chosen to express it as nmol GTP hydrolyzed per minute per μmol Toc protein. Since each substrate concentration has an associated rate, one can create a graph such that substrate concentration is on the x-axis and rate is on the y-axis; this is also known as a Michaelis–Menten plot. By applying the Michaelis–Menten equation, a nonlinear fit can be made and V_{max} and K_M can be determined.

Since it has been shown in the past that transit peptide was recognized and bound by Toc34 (Reddick *et al.*, 2007; Schleiff *et al.*, 2002), we incorporated it into our GTPase hydrolysis assay. Simply by performing several GTP titration experiments (as described above) and incorporating different concentrations of transit peptide in each GTP titration experiment, one can see that the CPM versus time graph indicates a greater release of radioactivity as a function of time for the different treatments (Fig. 7A), indicating that a greater amount of hydrolysis is occurring per unit time. After determining these linear rates (in ΔCPM/min) and applying the calculation in Eq. (2), one can determine the V_{max} and K_M of psToc34 in the presence of transit peptide, prSSU and mSSU and compare this to the previous enzymatic parameters in its absence (Fig. 7B). This allowed us in 2007 to determine how the transit peptide increases the overall hydrolytic rate of psToc34 while concomitantly decreasing the K_M (increasing the affinity for substrate). This represents the first time that a GAP, or GTPase Activating Protein, was identified for the Toc GTPases (Reddick *et al.*, 2007).

C. GTP Binding Assay

The 96-well nucleotide competition binding experiment relies on the capture of His-tagged Toc proteins bound to magnetic Ni–NTA agarose beads (Qiagen Inc. Valencia, California) via a hybrid plate magnet developed by the Joint Genome Institute at Lawrence Berkeley National Laboratory (Humphries *et al.*, 2004). This

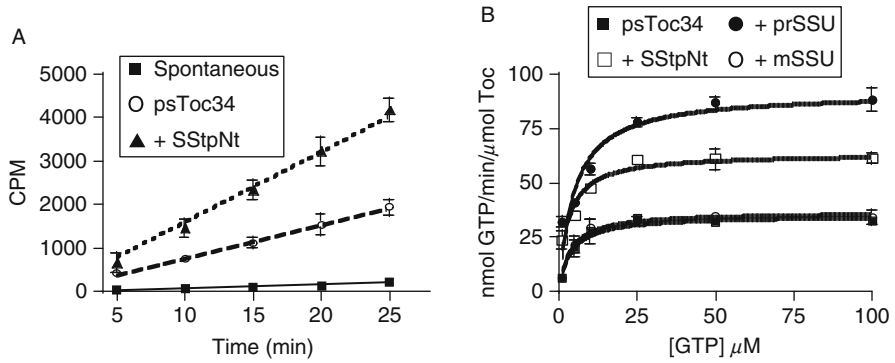

Fig. 7 Panel A shows the evolution of $^{32}P_i$ per unit time data generated by the hydrolysis assay. For simplicity, three traces are shown, each at 25 μM GTP; if an entire experiment were shown, low [GTP] has a large slope whereas high [GTP] has a lower slope due to the ratio of [Hot] to [Cold] in each well. The slope of the spontaneous is very small, whereas the slope of the psToc34 + SStpNt indicates a higher rate of hydrolysis as compared to psToc34 alone. Panel B shows the data after the activity calculation (Eq. 1). psToc34 has a basal rate of ~35 nmol GTP/min/μmol Toc, and is unchanged by the addition of mSSU. However, the addition of SStpNt increases the V_{max} to ~65 nmol/min/μmol and prSSU further increases that rate to ~90 nmol/min/μmol indicating that portions of prSSU may also stimulate the hydrolytic rate.

$$\text{Activity} = \frac{C_m I_m R_{GTP} S_f}{D_m M_{Toc} C_{dil} C_{eff} P_f}$$

Eq. 2 GTPase Activity Calculation. Specific activity of Toc protein, measured in nmol GTP hydrolyzed per minute per mol Toc. C_m, Δcpm/min; I_m, isotope/time point; R_{GTP}, Ratio (cold:hot) GTP; S_f, scintillation fraction factor; D_m, dpm/time point; M_{Toc}, Toc molecules; C_{dil}, HCl/charcoal dilution factor; C_{eff}, counting efficiency; P_f, isotope purity factor

assay was developed in order to accurately and quantitatively determine the K_d and K_i for the Toc GTPases and was first published in 2007 (Reddick *et al.*, 2007).

1. A 25 μl serial dilution of unlabeled competitor is performed across the 96-well plate such that each row of wells is either a different competitor, or each competitor is represented twice on the plate for duplicate analysis.

2. A constant volume of 25 μl (of various concentrations per experiment[2]) of 3000 Ci/mmol [α-^{32}P]GTP is added to all wells.

3. Ni–NTA magnetic agarose beads are incubated with the His-tagged Toc protein of choice on ice to allow sufficient affinity binding. A 50 μl suspension of magnetic beads and enzyme is added to each well of the 96-well plate to start the reaction.

4. Allow the reaction to proceed for 30 min on ice. Place the 96-well reaction plate on a 96-well plate magnet. This will draw down the magnetic beads and allow efficient washing of the plate. Wash with a volume of 300 μl 1× GBS buffer with

[2] The author recommends performing, at minimum, 3 plate experiments with varying [α-^{32}P]GTP to determine an appropriate amount for global fit analysis.

either a continual microplate washer or repeated pipetting of buffer manually for 2–3 min. This will remove all nonspecific background counts.

5. While still on the magnetic plate, aspirate to near dryness without disturbing the Ni–NTA beads.

6. Add 100 μl 500 mM imidazole in GBS buffer, remove plate from magnet, and allow to incubate for 10 min on ice with gentle agitation.

7. Place the 96-well plate back onto the magnet for 5 min to ensure complete draw down of the magnetic beads and remove 20 μl of the reaction mixture to a TopCount MicroScintillation Plate containing 100 μl MicroScint 40 scintillation fluid.

8. Repeat step 9 from the GTP Hydrolysis Assay.

This highly quantitative assay was employed to determine the K_d (GTP) and the K_i (various nucleotides and analogues) for four Toc proteins: atToc33, atToc34, psToc34, and atToc159G (Reddick *et al.*, 2007). Presented here are the binding curves of GTP and GDP to psToc34 (Fig. 8A). In order to avoid ambiguous results common with homologous competition experiments, the assay was repeated twice with different initial [α-^{32}P]GTP concentrations and all data was fit using the GlobalFit parameters in GraphPad Prism 4.0c. Using this experimental procedure, we generate 12 data sets per global fit analysis: two replicates, each counted in triplicate at two different [α-^{32}P]GTP concentrations. These data are fit to Eq. (3) (K_d) with the log K_d value shared for global fitting and the amount of hot and cold nucleotide constrained according to the above protocol. For heterologous binding competitions to determine K_i, the experiments are set up in the same manner with

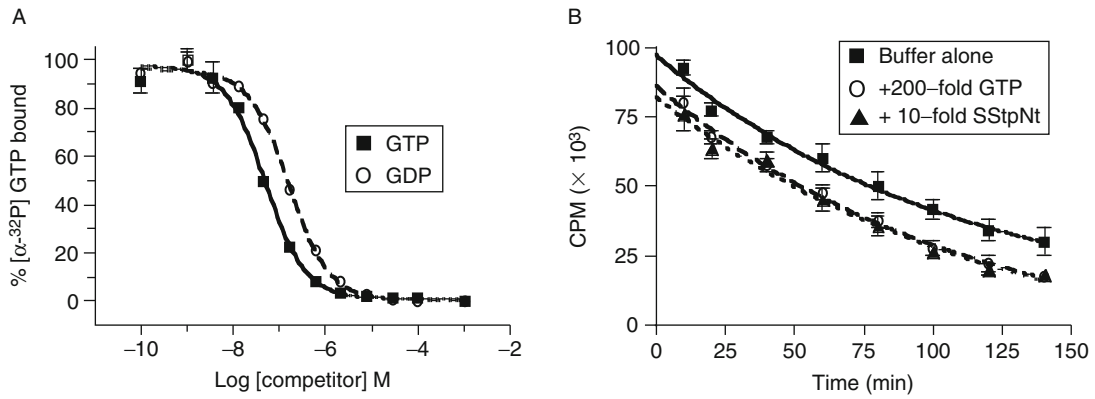

Fig. 8 Quantitative GTP binding and GTP/GDP exchange assays. Panel A shows data obtained from a binding experiment and reports the K_d of GTP (~50 nM) and the K_i of GDP (~151 nM). Panel B indicates the loss of bound [α-^{32}P]GTP over time (squares, solid line) and the addition of 200-fold [GTP] (circles, dashed line) only modestly increases this rate. Finally, the addition of 200-fold [GTP] with 10-fold [transit peptide] (triangles, dotted line) does not increase this rate of exchange.

$$\text{Total Binding} = \frac{B_{\max}[Hot]}{[Hot] + [Cold] + K_d} + NS$$

Eq. 3 K_d Calculation. Total Binding is defined as the non specific counts (NS) plus the ratio of the product of the maximal binding of GTP (B_{max}) and the concentration of the radioactive nucleotide ([Hot]) in the assay divided by the sum of the radioactive nucleotide concentration, cold competitor ([Cold]) and the dissociation constant (Kd)

the analysis fit to Eq. (4). In the case of measuring K_i, one must first determine K_d and use that value in order to determine K_i. The value for K_i was shared in the global fit and the amount of labeled and unlabeled GTP remained constant. For data analysis, 95% confidence is recommended.

D. *In vitro* Toc GTPase Nucleotide Exchange Assay

As a general rule, GTP-binding proteins have a very low basal hydrolytic rate and for efficient hydrolysis they require interaction with a GAP in order to accelerate the GTP cleavage step. The transit peptide acts as a GAP for psToc34, but a GEF protein has not yet been identified. Our nucleotide binding assay, described above, was modified such that a GEF experiment could be performed.

1. Toc protein is incubated with an excess of [α-^{32}P]GTP over night at 10 °C.
2. The protein is desalted on a PD-10 column (BD Biosciences) equilibrated with 1× GBS buffer in order to remove unbound GTP.
3. Similar to the GTP binding experiment earlier, the Toc protein is incubated with Ni–NTA magnetic agarose beads for ~1 h to allow affinity binding. The affinity bound protein and magnetic bead slurry is adjusted to 200 nM Toc protein and 50 μl is aliquoted into each well of a 96-well plate.
4. The time course of dissociation of bound radiolabeled nucleotide is started with the 50 μ1 addition of either GBS, GBS + 100-fold BSA, GBS + 100-fold cold GTP, GBS + various concentrations of transit peptide (or any other suspected GEF). Each column of the 96-well plate represents a time point, while each row of the plate represents an experimental condition.
5. At time = 10 min the plate is placed on the 96-well plate magnet and column 1 is washed three times with 200 μ1 GBS buffer. Then 200 μ1 500 mM imidazole in GBS buffer is added and incubated for 10 min off the magnet with gentle agitation.

$$\text{Total Binding} = \frac{B_{\max}[Hot]}{[Hot] + K_d\left(1 + \frac{[Cold]}{K_i}\right)}$$

Eq. 4 K_i Calculation. Total Binding is defined as the ratio of the product of the maximal binding of GTP (B_{max}) and the concentration of the radioactive nucleotide in the assay ([Hot]) divided by the sum of the radioactive nucleotide concentration and the product of the dissociation constant (K_d) and 1+ the cold nucleotide competitor concentration ([Cold]) over the inhibition constant (K_i)

6. The plate is placed back on the magnet, and 20 μ1 from 1A–H in the reaction plate is removed to 1A–H of a TopCount MicroScintillation Plate containing 100 μ1 MicroScint 40 scintillation fluid.
7. This procedure is repeated every 10 min for each following column such that column 2 = 20 min; 3 = 30 min; 4 = 40 min, etc.
8. Once the assay is complete, repeat step 9 from the GTP Hydrolysis Assay.

The GTPase assay indicated that transit peptides stimulate the V_{max} and lowered the K_M while the GEF assay indicated that transit peptide does not stimulate the exchange reaction, Fig. 8B. This allowed us to conclude that the transit peptide is indeed the GAP for psToc34, however to date, no GEF has been identified. It is possible that other Toc components or even 14–3–3 proteins and chaperones could be the GEF for psToc34. This GTP/GDP exchange assay will afford us the opportunity to determine the answer to that question in a very quantitative manner.

V. Molecular Modeling of Toc Proteins

A. Introduction to Toc75 and POTRA Domains

Toc75 falls into a broad category known as the outer-membrane protein family (OMPs) that are folded and inserted into membranes by a process conserved between prokaryotes and eukaryotes (Paschen *et al.*, 2003; Reumann *et al.*, 1999). The central transmembrane component is a highly conserved β-barrel protein; members of this family of proteins are involved in protein translocation into and across the outer membrane of gram negative bacteria (Omp85/YaeT), chloroplast (Toc75), and mitochondria (Sam50/Tob55) (Gentle *et al.*, 2005).

Folded soluble domains at the termini of β-barrel proteins have been involved in recognizing peptides or other unstructured proteins as substrates for translocation (Gentle *et al.*, 2005). These polypeptide transport associated (POTRA) domains are present in three copies in the Toc75 protein (Sanchez-Pulido *et al.*, 2003). Using HMMer to perform Hidden Markov Profile searches and the HMM profiles of POTRA2 and the related Bacterial Surface Antigen (both downloaded from the pFam database, Sanger Institute), the POTRA domains of psToc75 were identified as POTRA1, residues 161–237, POTRA2, residues 266–355, and POTRA3 residues 366–439 (all residue numbers correspond to the preprotein, that is, 131 residues in transit peptide (Ertel *et al.*, 2005)). Although the C-terminal, β-barrel portion of psToc75 is >75% similar to FhaC, an Omp-related protein of known structure (Fig. 9A), the N-terminal portion has little similarity. However, with the POTRA domains already identified, there is adequate information to give a reasonable homology model including POTRA 2 and 3 as well as the β-barrel, Fig. 9B. Modeller 9v2 (Eswar *et al.*, 2008) was used along with alignments generated by align2d (also in the Modeller package) and hand edited to properly align the POTRA domains as identified by HMMer, Fig. 9C and D. Since the results of the modeling were reasonable, the POTRA domains were subsequently cloned and purified via IMPACT system (Fig. 10A), as discussed previously in IIB. After obtaining purified

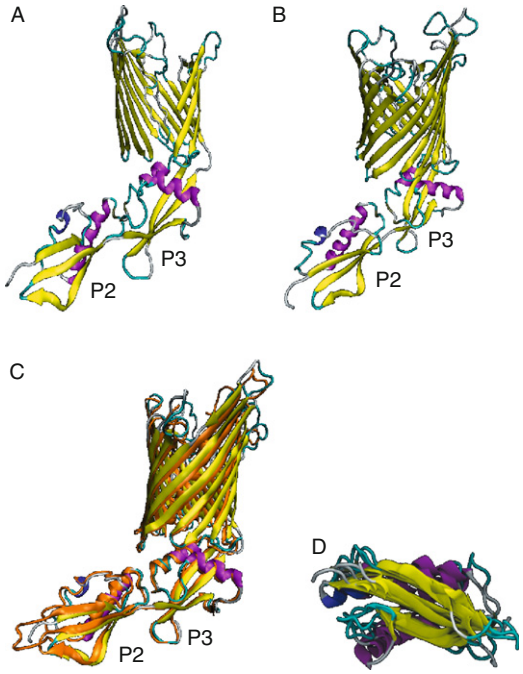

Fig. 9 Structural modeling of Toc75 and POTRA domains. Panel A shows the structure of FhaC (Clantin *et al.*, 2007). Panel B is the structural estimation of Toc75 based on the structure of FhaC; only POTRA 2 and 3 are modeled since FhaC only has 2 POTRA domains on which to model. Panel C shows the superimposition of the FhaC and Toc75 models; in panels A–C P2 and P3 refer to PORTA 2 and 3, respectively. Panel D, two POTRA domains of FhaC and the four POTRA domains of YaeT from *Bordetella pertussis* and *E. coli,* respectively, are easily super-imposable indicating a high degree of structural similarity. The fold in each domain revealed the presence of three-stranded β-sheets and two helices. The β-strands are labeled in yellow and the helices are labeled in purple; the loops are shown in light blue.

POTRA, we analyzed the overall fold of the POTRA domain using circular dichroism spectroscopy and determined that it was folded as predicted as compared to observed secondary structure of the six known POTRA structures, seen in Fig. 10B and summarized in Fig. 10C. Here we show purified psToc75-POTRA1 and CD spectra confirming reasonable amounts of each secondary structural element. This and the other purified POTRA domains will make critical tools for further quantitative inquiries into the function of the TOC apparatus.

VI. Conclusions and Perspectives

The chloroplast import apparatus is a remarkable nanoscale molecular gate and molecular motor. The Toc translocon is responsible for distinguishing between thousands of soluble cytosolic proteins and selecting only those containing an

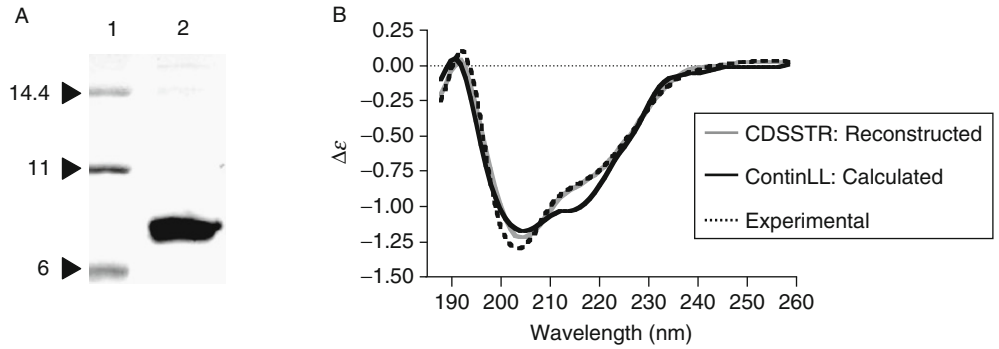

C

Comparison of psTOC75-POTRA1 with known POTRA secondary structures

	YaeT				FhaC			psToc75
Structural elements	Potra 1	Potra 2	Potra 3	Potra 4	Potra1	Potra 2	Average	Potra 1
Helix	0.29	0.33	0.30	0.32	0.28	0.20	0.27 ± 0.05	0.06
Strand	0.37	0.33	0.35	0.31	0.35	0.29	0.33 ± 0.03	0.33
Turn	0.16	0.23	0.22	0.23	0.23	0.39	0.26 ± 0.09	0.24
Unordered	0.19	0.12	0.14	0.14	0.14	0.12	0.14 ± 0.02	0.37

Fig. 10 POTRA production, and secondary structural analysis. Panel A shows purified POTRA 1 from subcloning; lane 1 is markers, listed at the left in kDa and 2 is the purified POTRA protein. Panel B is the experimental CD spectra of POTRA graphed with the theoretical CD spectra of two different secondary structure estimation tools (CDSSTR and ContinLL). Panel C represents the deconvolution of CD spectra and provided an estimation of the secondary structure of observed data which compares with the residues of the calculated composition of the average of the four *E. coli YaeT* and the two *B. pertussis* POTRA domains.

N-terminal transit peptide for import. This activity is sufficiently robust to enable the rapid development of chloroplasts in only a few days during the greening process of adolescent plants (Pilon *et al.*, 1992). *In vitro* analysis has demonstrated that the Toc apparatus can import proteins on the order 40,000 molecules per chloroplast per minute (Cline *et al.*, 1993), however despite this remarkable activity, neither the mechanism of preprotein selection nor the process of preprotein translocation is well understood. This chapter describes some of the current methods used in our laboratory to explore the activity and dynamics of the Toc apparatus *in vitro* and *in organeller*.

We describe the isolation and purification of chloroplasts in order to perform highly quantitative binding and import assays which have helped us to accurately determine the K_d and K_i of prSSU and nonprSSU competitors for binding (i.e., mutants of prSSU) as well as the IC_{50} of prSSU for import. Additionally, the solubilization of the Toc translocon from intact chloroplasts was described, after

which BN-PAGE separates the complexes according to native size and 2-D PAGE separates the individual components according to nominal molecular mass. This technique lends itself very well to Western analysis where we can decipher translocon components and estimate stoichiometry. By employing this technique, our laboratory has been afforded the opportunity to perform translocon solubilization under a host of conditions (the addition of prSSU, mSSU, transit peptide, as well as various nucleotide loading states) to understand how the dynamics of this complex are related to substrates and nucleotides. Utilizing a novel $^{32}P_i$ activated charcoal filter assay, we have accurately determined the V_{max} and K_M of Toc proteins under a host of conditions. Next, with the use of a magnetic affinity capture technique, we can determine the K_d and K_i of GTP and other various nucleotides as well as perform GTP/GDP exchange experiments. Finally, through the use of molecular modeling and circular dichroism spectroscopy, we have estimated and confirmed the secondary structure of POTRA domains of the β-barrel protein Toc75. These domains have therefore been implicated as important portions of the protein and are most likely involved in the overall process of protein translocation into the chloroplast. Fig. 11 artistically indicates that through these quantitative techniques, we can visualize the transit peptide bound to the chloroplast surface and show that the inner and outer chloroplast membranes come together to facilitate Toc–Tic interaction and import, which on the most nanoscale represents the transit peptide's interactions with the Toc subunits which ultimately facilitate import.

Future Directions and Opportunities: Future work in chloroplast protein import will benefit from not only the quantitative methods that we describe above but also from other areas of biology that are rapidly developing. For example, as a result of high throughput crystallography efforts, the availability of new and potentially related structures is growing. This resource as well as new computational tools permit homology modeling of Toc subunits with higher confidence, which in turn, allows for the current design of powerful experiments prior to the successful determination of the structure of the Toc translocon. Our ability to estimate the structure of the POTRA domains of psToc75 through *in silico* methodology is one example of such modeling progress.

Another opportunity is linked to the wealth of new genomic resources and genomic tools. Recent progress has been made in predictive algorithms that can predict chloroplast localized proteins based on analysis of their N-terminal sequence. Recently, a new tool, the transit peptide prediction program MultiP (http://sbi.postech.ac.kr/MultiP/), has been developed (Lee *et al.*, 2008) that reports an accuracy of ~94% which is considerably better than ChloroP (77%) which has been the most popular tool used to date (Emanuelsson *et al.*, 1999). In addition, the number of new plant and algal genomes is rapidly expanding. There are five currently available plastid containing genomes as either completed or in draft form with another eight in progress (Rubin, 2008). As these genomes become available, the identification and analysis of the plastid predicted proteome will provide new information on the metabolic role of the chloroplast as well as provide new insight into the structure and diversity of transit peptides.

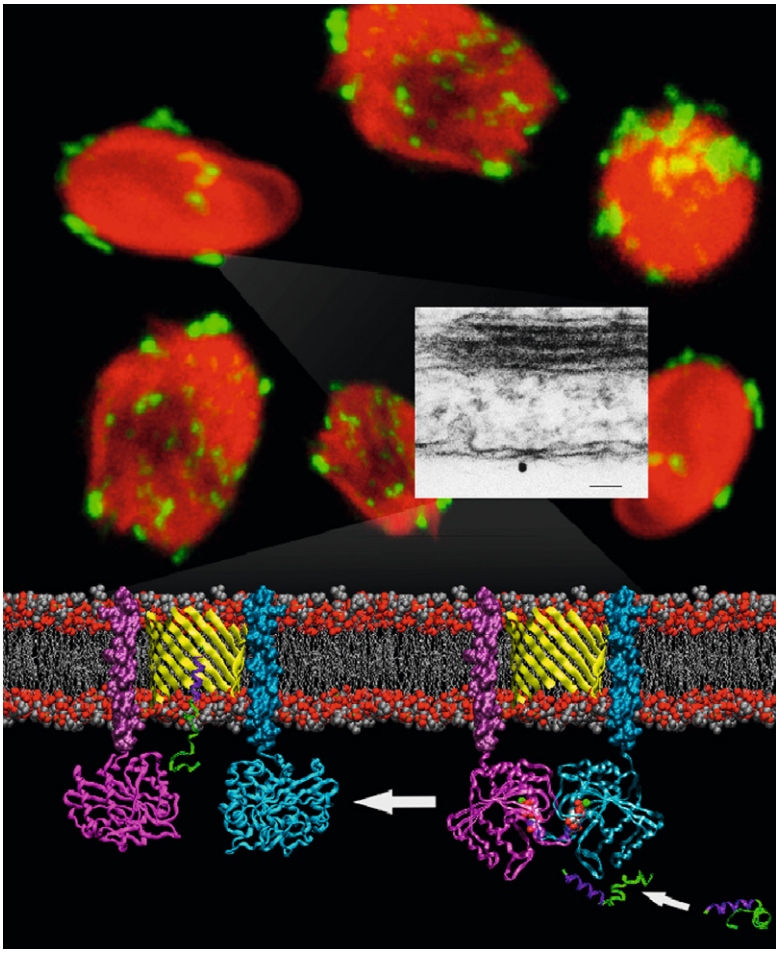

Fig. 11 The big picture. Chloroplasts appearing red in color due to the inflorescence of chlorophyll are immunodecorated with FITC-conjugated antibodies against bound transit peptide. When visualized using electron microscopy (insert), the bound transit peptide is identified using an antibody conjugated to a nano-gold particle (for detection with EM) and implies that translocation across the outer and inner membranes of the chloroplast occur simultaneously. Finally, using molecular modeling, we hypothesize on the molecular dynamics involved with transit peptide recognition by members of the Toc translocon, which lead to protein import.

Acknowledgments

We would like to thank Ian M. Campbell for his assistance with Fig. 1. We are appreciative of the technical expertise of Dr. John Biggerstaff and his undergraduate student Bill McCartt in the analysis of the TIRF data. We also thank Dr. Chitra Subramanian and Mr. Anton V. Mitsky for their assistance with analysis of His-S-SStpNt. Jeffrey D. Whyte at MP Biomedical has continued to provide excellent service and support. We received support from the NSF program in Cell Biology; award numbers MCB0628670 and MCB0344601.

References

Arnon, D. I. (1949). Copper enzymes in isolated chloroplasts. Polyphenoloxidase in beta vulgaris. *Plant Physiol.* **24,** 1–15.

Axelrod, D. (2001). Selective imaging of surface fluorescence with very high aperture microscope objectives. *J. Biomed. Opt.* **6,** 6–13.

Basu, M. K., Rogozin, I. B., Deusch, O., Dagan, T., Martin, W., and Koonin, E. V. (2008). Evolutionary dynamics of introns in plastid-derived genes in plants: Saturation nearly reached but slow intron gain continues. *Mol. Biol. Evol.* **25,** 111–119.

Beckmann, R., Spahn, C. M., Eswar, N., Helmers, J., Penczek, P. A., Sali, A., Frank, J., and Blobel, G. (2001). Architecture of the protein-conducting channel associated with the translating 80S ribosome. *Cell* **107,** 361–372.

Bolter, B., Soll, J., Schulz, A., Hinnah, S., and Wagner, R. (1998). Origin of a chloroplast protein importer. *Proc. Natl. Acad. Sci. USA.* **95,** 15831–15836.

Bos, J. L., Rehmann, H., and Wittinghofer, A. (2007). GEFs and GAPs: Critical elements in the control of small G proteins. *Cell* **129,** 865–877.

Bourne, H. R., Sanders, D. A., and McCormick, F. (1990). The GTPase superfamily: A conserved switch for diverse cell functions. *Nature.* **348,** 125–132.

Bourne, H. R., Sanders, D. A., and McCormick, F. (1991). The GTPase superfamily: Conserved structure and molecular mechanism. *Nature.* **349,** 117–127.

Bruce, B. D. (2000). Chloroplast transit peptides: Structure, function and evolution. *Trends Cell Biol.* **10,** 440–447.

Caliebe, A., Grimm, R., Kaiser, G., Lubeck, J., Soll, J., and Heins, L. (1997). The chloroplastic protein import machinery contains a Rieske-type iron-sulfur cluster and a mononuclear iron-binding protein. *EMBO J.* **16,** 7342–7350.

Cavalier-Smith, T. (2003). Genomic reduction and evolution of novel genetic membranes and protein-targeting machinery in eukaryote-eukaryote chimaeras (meta-algae). *Philos. Trans. R. Soc. Lond. B, Biol. Sci.* **358,** 109–133.

Chen, K. Y., and Li, H. M. (2007). Precursor binding to an 880-kDa Toc complex as an early step during active import of protein into chloroplasts. *Plant J.* **49,** 149–158.

Clantin, B., Delattre, A. S., Rucktooa, P., Saint, N., Méli, A. C., Locht, C., Jacob-Dubuisson, F., and Villeret, V. (2007 Aug 17). Structure of the membrane protein FhaC: a member of the Omp85-TpsB transporter superfamily. *Science* **317,** 957–961.

Cline, K., Henry, R., Li, C., and Yuan, J. (1993). Multiple pathways for protein transport into or across the thylakoid membrane.. *EMBO J.* **12,** 4105–4114.

Dekker, P. J., Muller, H., Rassow, J., and Pfanner, N. (1996). Characterization of the preprotein translocase of the outer mitochondrial membrane by blue native electrophoresis. *Biol. Chem.* **377,** 535–538.

Dekker, P. J., Ryan, M. T., Brix, J., Muller, H., Honlinger, A., and Pfanner, N. (1998). Preprotein translocase of the outer mitochondrial membrane: Molecular dissection and assembly of the general import pore complex. *Mol. Cell Biol.* **18,** 6515–6524.

Emanuelsson, O., Nielsen, H., and von Heijne, G. (1999). ChloroP, a neural network-based method for predicting chloroplast transit peptides and their cleavage sites. *Protein Sci.* **8,** 978–984.

Ertel, F., Mirus, O., Bredemeier, R., Moslavac, S., Becker, T., and Schleiff, E. (2005). The evolutionarily related beta-barrel polypeptide transporters from *Pisum sativum* and Nostoc PCC7120 contain two distinct functional domains. *J. Biol. Chem.* **280,** 28281–28289.

Eswar, N., Eramian, D., Webb, B., Shen, M. Y., and Sali, A. (2008). Protein structure modeling with MODELLER. *Methods Mol. Biol.* **426,** 145–159.

Eubel, H., Braun, H. P., and Millar, A. H. (2005). Blue-native PAGE in plants: A tool in analysis of protein–protein interactions. *Plant Methods.* **1,** 11.

Gentle, I. E., Burri, L., and Lithgow, T. (2005). Molecular architecture and function of the Omp85 family of proteins. *Mol. Microbiol.* **58,** 1216–1225.

Humphries, D., Pollard, M., Elkin, C., Petermann, K., Reiter, C., and Cepeda, M. (2004). New high performance magnet structures for bead based molecular separation. *Lawrence Berkeley Natl. Lab. Rep.* **58894,** 1–12.

Jarvis, P., and Soll, J. (2001). Toc, Tic, and chloroplast protein import. *Biochim. Biophys. Acta.* **1541,** 64–79.

Keegstra, K., and Cline, K. (1999). Protein import and routing systems of chloroplasts. *Plant Cell.* **11,** 557–570.

Kikuchi, S., Hirohashi, T., and Nakai, M. (2006). Characterization of the preprotein translocon at the outer envelope membrane of chloroplasts by blue native PAGE. *Plant Cell Physiol.* **47,** 363–371.

Kim, J. S., and Raines, R. T. (1993). Ribonuclease S-Peptide as a carrier in fusion proteins. *Protein Sci.* **2,** 348–356.

Kleffmann, T., Hirsch-Hoffmann, M., Gruissem, W., and Baginsky, S. (2006). plprot: A comprehensive proteome database for different plastid types. *Plant Cell Physiol.* **47,** 432–436.

Klein, R. R., and Salvucci, M. E. (1992). Photoaffinity labeling of mature and precursor forms of the small subunit of RIBULOSE-1,5-Bisphosphate carboxylase/oxygenase after expression in *Escherichia coli*. *Plant Physiol.* **98,** 546–553.

Kuchler, M., Decker, S., Hormann, F., Soll, J., and Heins, L. (2002). Protein import into chloroplasts involves redox-regulated proteins. *EMBO J.* **21,** 6136–6145.

Lee, D. W., Kim, J. K., Lee, S., Choi, S., Kim, S., and Hwang, I. (2008). Arabidopsis nuclear-encoded plastid transit peptides contain multiple sequence subgroups with distinctive chloroplast-targeting sequence motifs. *Plant Cell.* **20,** 1603–1622.

Meisinger, C., Ryan, M. T., Hill, K., Model, K., Lim, J. H., Sickmann, A., Muller, H., Meyer, H. E., Wagner, R., and Pfanner, N. (2001). Protein import channel of the outer mitochondrial membrane: A highly stable Tom40-Tom22 core structure differentially interacts with preproteins, small tom proteins, and import receptors. *Mol. Cell Biol.* **21,** 2337–2348.

Model, K., Meisinger, C., and Kuhlbrandt, W. (2008). Cryo-Electron microscopy structure of a yeast mitochondrial preprotein translocase. *J. Mol. Biol.* **383,** 1049–1057.

Olsen, L. J., Theg, S. M., Selman, B. R., and Keegstra, K. (1989). ATP is required for the binding of precursor proteins to chloroplasts. *J. Biol. Chem.* **264,** 6724–6729.

Paschen, S. A., Waizenegger, T., Stan, T., Preuss, M., Cyrklaff, M., Hell, K., Rapaport, D., and Neupert, W. (2003). Evolutionary conservation of biogenesis of beta-barrel membrane proteins. *Nature* **426,** 862–866.

Pilon, M., Weisbeek, P. J., and de Kruijff, B. (1992). Kinetic analysis of translocation into isolated chloroplasts of the purified ferredoxin precursor. *FEBS Lett.* **302,** 65–68.

Reddick, L. E., Vaughn, M. D., Wright, S. J., Campbell, I. M., and Bruce, B. D. (2007). *In vitro* comparative kinetic analysis of the chloroplast Toc GTPases. *J. Biol. Chem.* **282,** 11410–11426.

Reumann, S., Davila-Aponte, J., and Keegstra, K. (1999). The evolutionary origin of the protein-translocating channel of chloroplastic envelope membranes: Identification of a cyanobacterial homolog. *Proc. Natl. Acad. Sci. USA* **96,** 784–789.

Rubin, E. M. (2008). Genomics of cellulosic biofuels. *Nature* **454,** 841–845.

Sanchez-Pulido, L., Devos, D., Genevrois, S., Vicente, M., and Valencia, A. (2003). POTRA: A conserved domain in the FtsQ family and a class of beta-barrel outer membrane proteins. *Trends Biochem. Sci.* **28,** 523–526.

Schagger, H., and von Jagow, G. (1991). Blue native electrophoresis for isolation of membrane protein complexes in enzymatically active form. *Anal. Biochem.* **199,** 223–231.

Schagger, H., Cramer, W. A., and von Jagow, G. (1994). Analysis of molecular masses and oligomeric states of protein complexes by blue native electrophoresis and isolation of membrane protein complexes by two-dimensional native electrophoresis. *Anal. Biochem.* **217,** 220–230.

Schleiff, E., Soll, J., Sveshnikova, N., Tien, R., Wright, S., Dabney-Smith, C., Subramanian, C., and Bruce, B. D. (2002). Structural and guanosine triphosphate/diphosphate requirements for transit peptide recognition by the cytosolic domain of the chloroplast outer envelope receptor, Toc34. *Biochemistry* **41,** 1934–1946.

Schleiff, E., Soll, J., Kuchler, M., Kuhlbrandt, W., and Harrer, R. (2003). Characterization of the translocon of the outer envelope of chloroplasts. *J. Cell Biol.* **160,** 541–551.

Subramanian, C., Ivey, R., and Bruce, B. D. (2001). Cytometric analysis of an epitope-tagged transit peptide bound to the chloroplast translocation apparatus. *Plant J.* **25,** 349–363.

Theg, S. M., Bauerle, C., Olsen, L. J., Selman, B. R., and Keegstra, K. (1989). Internal ATP is the only energy requirement for the translocation of precursor proteins across chloroplastic membranes. *J. Biol. Chem.* **264,** 6730–6736.

Toomre, D., and Manstein, D. J. (2001). Lighting up the cell surface with evanescent wave microscopy. *Trends Cell Biol.* **11,** 298–303.

Van den Berg, B., Clemons, W. M., Jr., Collinson, I., Modis, Y., Hartmann, E., Harrison, S. C., and Rapoport, T. A. (2004). X-ray structure of a protein-conducting channel. *Nature* **427,** 36–44.

Vetter, I. R., and Wittinghofer, A. (2001). The guanine nucleotide-binding switch in three dimensions. *Science* **294,** 1299–1304.